Rolling Bearing Fault Feature Extraction Using Local Maximum Synchrosqueezing Transform and Global Fuzzy Entropy

Keheng Zhu, Xiucheng Yue, Dejian Sun, Shichang Xiao and Xiong Hu

School of Logistics Engineering, Shanghai Maritime University, Shanghai 201306, China.
E-mail: hxshmtu@126.com

To achieve good performance of fault feature extraction for a rolling bearing, a new feature extraction method is presented in this paper based on local maximum synchrosqueezing transform (LMSST) and global fuzzy entropy (GFuzzyEn). First, targeting the time-varying features of the vibration signals of the rolling bearing, the LMSST algorithm, which is a newly developed time-frequency method and allows for adaptive mode decomposition, is used to preprocess the vibration signals into a number of mode components. Then, as a modification of FuzzyEn, GFuzzyEn is adopted to evaluate the complexity of these mode components. Compared to FuzzyEn, which focuses mainly on the local characteristics of the short-term physiological time series, the GFuzzyEn emphasizes the global characteristics of the signal considering that the bearing vibration signals' global fluctuation may change as the bearing works under various conditions. Finally, the fault features of the bearing vibration signals are extracted by combining the LMSST and the GFuzzyEn. The experimental analysis shows that the proposed LMSST-GFuzzyEn method can extract rich fault-related information from the bearing vibration data and can achieve good classification performance for rolling bearing fault diagnosis.

1. INTRODUCTION

The rolling bearing is a very crucial element of rotating machines in modern industry and plays a vital role in guaranteeing the steady operation of the whole machine system.[1–3] Therefore, it is of great significance to fulfill a rolling bearing fault diagnosis for an avoidance of a mechanical failure. The vibration analysis is one of the most extensively and effectively used approaches for fault diagnosis of a rolling bearing because rich information about the bearing's working condition is hidden in the vibration signals.[4–7]

Feature extraction from the vibration signals is a critical step in the fault diagnosis of rolling bearings, which directly influences the identification accuracy of different bearing running states. Focusing on the time-varying features of bearing vibration signals, a number of time-frequency (TF) analysis (TFA) methods have been proposed to preprocess the vibration signals for fault feature extraction of rolling bearings, among which the empirical mode decomposition (EMD) algorithm developed by Huang et al.[8] has been the one most widely used in the bearing fault feature extraction field.[9–11] However, there exists a mode mixing problem in EMD and it lacks theoretical foundation,[12] which limits the application of EMD. Another commonly used TF technique is the synchrosqueezing transform (SST) algorithm. The SST algorithm not only enhances the TF resolution but also can achieve precise signal reconstruction.[13, 14] Therefore, the SST method has been successfully applied in the bearing fault diagnosis field.[15, 16] However, the TF representation energy obtained from SST smears seriously when the strongly frequency-modulated (FM) signals are addressed. In order to deal with this problem, a novel SST approach called local maximum synchrosqueezing transform (LMSST) is proposed.[17] Compared with the original SST, the LMSST can produce a more highly concentrated TF represen-

tation. At the same time, the perfect signal reconstruction and adaptive mode decomposition can be both realized. Considering these merits, the LMSST method is utilized in this paper as a pretreatment of extracting fault features from the vibration signals of rolling bearings.

After the raw vibration signal is decomposed, it is necessary to further process the decomposition mode components for fault feature extraction. During recent years, in view of the suitability of analyzing the nonlinear time series, some entropy-based nonlinear dynamics parameters have been introduced to extract fault information from the bearing vibration signals, such as appropriate entropy (ApEn),[18] sample entropy (SampEn),[19–22] and fuzzy entropy (FuzzyEn).[23–25] The definition change of the three kinds of entropy is a process of gradual improvement. The ApEn algorithm proposed by Pincus[26] is designed to measure the complexity of time sequence, but its computation is influenced greatly by the data length and it uniformly has a lower corresponding estimated value than the expected one.[27] SampEn is developed by Richman and Moorman[27] to overcome the shortcomings of ApEn, which can achieve better results than ApEn when evaluating the signals' complexity. Nevertheless, in both SampEn and ApEn, the similarity degree between vectors is defined based on Heaviside function. However, the Heaviside function has a rigid and discontinuous boundary while most classes have ambiguous boundaries in the real applications. In order to address this problem, Chen et al.[28] put forward a new fuzzy entropy (FuzzyEn) method by replacing the Heaviside function with the fuzzy function. Because of the continuous boundaries of the fuzzy function, FuzzyEn exhibits a better statistical stability than SampEn and can measure the complexity of the signals more accurately. However, FuzzyEn only emphasizes the signals' local characteristics while ignoring the corresponding

global fluctuation. To this end, Liu et al.[29] presented a new fuzzy entropy approach, which considers both the local and the global characteristics of the signal at the same time. Considering that FuzzyEn focuses mainly on the short-term physiological signals and their local characteristics and was inspired by the idea of Liu, the global fuzzy entropy (GFuzzyEn) is introduced to evaluate the complexity of the bearing vibration signals, in which the local mean used in FuzzyEn is replaced by the global mean in the procedure of vector generalization. In this paper, GFuzzyEn is employed to process the mode components decomposed by LMSST for the accomplishment of the feature extraction.

In this study, a fault feature extraction approach is proposed based on LMSST and GFuzzyEn. First, the bearing vibration signals under different working conditions are decomposed by LMSST into a series of mode components. The GFuzzyEn algorithm is then adopted to calculate the GFuzzyEn values of the LMSST components to complete the bearing fault feature extraction. Finally, the LMSST-GFuzzyEn features are used for fault diagnosis of a rolling bearing.

The paper is arranged as follows. The LMSST theory is briefly presented in Section 2. The introduction of GFuzzyEn is given in Section 3. In Section 4, the bearing fault feature extraction approach based on LMSST and GFuzzyEn is proposed. The simulation validation of the LMSST method is presented in Section 5. Section 6 presents the experimental validation of the proposed method. Finally, the conclusion is drawn in Section 7.

2. THE LOCAL MAXIMUM SYNCHRO-SQUEEZING TRANSFORM METHOD

The LMSST method starts with the framework of short time Fourier transform (STFT), which is defined by:

$$G(t,\omega) = \int_{-\infty}^{+\infty} g(u-t)s(u)e^{-i\omega(u-t)}du; \qquad (1)$$

where the signal $s \in L^2(\mathbb{R})$, the window $g \in L^2(\mathbb{R})$ and $s(t) = \sum_{k=1}^{n} A_k(t)e^{i\varphi_k(t)}$ is a multi-component signal with amplitude-modulation and frequency-modulation. The STFT can effectively extract the instantaneous amplitude (IA) and instantaneous frequency (IF) by expanding the 1D time-series signal into the 2D TF plane. To recover the original signal, inverse STFT can be used as:

$$\int_{-\infty}^{+\infty} G(t,\omega)d\omega = \int_{-\infty}^{+\infty}\int_{-\infty}^{+\infty} g(u-t)s(u)e^{-i\omega(u-t)}du\,d\omega =$$

$$2\pi \int_{-\infty}^{+\infty} g(u-t)s(u)\delta(u-t)du = 2\pi g(0)s(t). \qquad (2)$$

Then, the original signal $s(t)$ can be reconstructed by:

$$s(t) = \left(2\pi g(0)\right)^{-1} \int_{-\infty}^{+\infty} G(t,\omega)d\omega. \qquad (3)$$

If each mode of signal occupies distinct area in the TF domain, they will be well separated in the TF plane. Then, each

mode can be recovered through integrating the TF coefficients around the IF in frequency direction:

$$s_k(t) = \left(2\pi g(0)\right)^{-1} \int\limits_{|\omega-\varphi_k'(t)|\leq\Delta} \int G(t,\omega)d\omega. \qquad (4)$$

However, the STFT is limited in that the TF energy of its spectrogram smears seriously, and the smearing will result in low resolution. In order to present the TF features more accurately, the reassignment method (RM) is developed to improve the readability of TF representation, which is defined as:

$$RM(\nu,\eta) = \int_{-\infty}^{+\infty} |G(t,\omega)|\delta(\nu,\hat{\omega}(t,\omega))\delta(\eta-(t,\omega))dt\,d\omega; \tag{5}$$

where δ is the Dirac distribution, and $\hat{\omega}(t,\omega)$, $\hat{t}(t,\omega)$ are the reassignment operators, which can be respectively computed as:

$$\hat{\omega}(t,\omega) = \omega - Im\left(\frac{G^{g'}(t,\omega)}{G(t,\omega)}\right); \qquad (6)$$

$$\hat{t}(t,\omega) = t + Re\left(\frac{G^{tg}(t,\omega)}{G(t,\omega)}\right). \qquad (7)$$

From the perspective of geometry, the STFT spectrogram $|G(t,\omega)|$ is reassigned by the RM from the point (t,ω) to the newly computed TF position $(\hat{t}(t,\omega),\hat{\omega}(t,\omega))$. The RM is able to reassign all spectrogram energy into the IF trajectory[30] and thus can realize the ideal TF location. However, the RM algorithm employs the amplitude spectrum while neglecting the phase information, so it is unable to reconstruct the time-series signals.[31]

To deal with the drawback in the RM method for recovering the original signal, the SST method is introduced, which can be expressed as:

$$SST(t,\eta) = \int_{-\infty}^{+\infty} G(t,\omega)\delta(\eta-\omega_0(t,\omega))d\omega. \qquad (8)$$

Compared with RM, which reassigns the TF spectrogram $|G(t,\omega)|$ along frequency and time directions, SST reassigns the TF coefficients $G(t,\omega)$ along the frequency direction. Therefore, the signal can be recovered by:

$$s_k(t) = \left(2\pi g(0)\right)^{-1} \int\limits_{|\omega-\varphi_k'(t)|\leq ds} SST(t,\omega)d\omega; \qquad (9)$$

where ds represents the reconstruction bandwidth.

From the aforementioned analysis, we know that the RM method can achieve high resolution in the TF plane while the SST method can realize the full reconstruction of the original signal. In order to have these two advantages simultaneously, the LMSST method is put forward by reassigning all of the smeared TF coefficients into the IF trajectories along the frequency direction, in which a new frequency-reassignment operator is defined as:

$$\omega_m(t,\omega) = \begin{cases} \underset{\omega}{\mathrm{argmax}}\,|G(t,\omega)|, & \omega \in [\omega-\Delta, \omega+\Delta], \\ & \qquad\qquad \text{if } |G(t,\omega)| \neq 0; \\ 0, & \text{if } |G(t,\omega)| = 0; \end{cases}$$

$$(10)$$

where:

$$|G(t,\omega)| = \sum_{k=1}^{n} A_k(t)\hat{g}\big(\omega - \varphi_k'(t)\big). \tag{11}$$

Since the Fourier transform of the window function has its maximum value at zero, i.e., $\hat{g}(\omega) < \hat{g}(0)$, the reassignment operator can be denoted as:

$$\omega_m(t,\omega) = \begin{cases} \varphi_k'(t), & \text{if } \omega \in [\varphi_k'(t) - \Delta, \varphi_k'(t) + \Delta)]; \\ 0, & \text{otherwise.} \end{cases} \tag{12}$$

In order to obtain the signal reconstruction ability, the TF coefficients should be reassigned in the frequency direction. Thus, the LMSST method is defined as:

$$LMSST(t,\eta) = \int_{-\infty}^{+\infty} G(t,\omega)\delta\big(\eta - \omega_m(t,\omega)\big)d\omega. \tag{13}$$

Then the original signal can be reconstructed by:

$$s(t) = \big(2\pi g(0)\big)^{-1} \int_{-\infty}^{+\infty} LMSST(t,\omega)d\omega; \tag{14}$$

and each mode component can be obtained from the TF coefficients only in the IF trajectories of LMSST, which is defined as:

$$s_k(t) = \big(2\pi g(0)\big)^{-1} LMSST\big(t, \varphi_k'(t)\big)d\omega. \tag{15}$$

In contrast with RM and SST, the LMSST method has a more highly concentrated TF representation. Meanwhile, LMSST can achieve a perfect signal reconstruction and monocomponent mode decomposition. The detailed description about the LMSST algorithm can be found in Yu et al.[17]

3. THE GLOBAL FUZZY ENTROPY

3.1. Fuzzy Entropy

The calculation procedures of FuzzyEn are listed as follows:[28]

1. For a time sequence with N data point $\{u(i) : 1 \leq i \leq N\}$, compose the m-dimensional vectors $\mathbf{X}_i^m$ as:

$$\mathbf{X}_i^m = \{u(i), u(i+1), \ldots, u(i+m-1)\} - u_0(i)$$
$$1 \leq i \leq N - m + 1; \tag{16}$$

where $\mathbf{X}_i^m$ represents a new time sequence, and $u_0(i)$ is defined as:

$$u_0(i) = m^{-1} \sum_{j=0}^{m-1} u(i+j). \tag{17}$$

2. The definition of distance between sequences of $\mathbf{X}_i^m$ and $\mathbf{X}_j^m$ is expressed as:

$$d_{ij}^m = d[\mathbf{X}_i^m, \mathbf{X}_j^m] = $$
$$\max_{k \in [0, m-1]} \big| \big(u(i+k) - u_0(i)\big) - \big(u(j+k) - u_0(j)\big)\big|. \tag{18}$$

3. The computation of similarity degree D_{ij}^m can be performed with a fuzzy function:

$$D_{ij}^m = \mu(d_{ij}^m, r). \tag{19}$$

4. Define $\varphi_i^m(r)$ as:

$$\varphi_i^m(r) = (N - m - 1)^{-1} \sum_{j=1, j \neq i}^{N-m} D_{ij}^m. \tag{20}$$

5. Denote the function $\varphi^m(r)$

$$\varphi^m(r) = (N - m)^{-1} \sum_{i=1}^{N-m} \varphi_i^m(r). \tag{21}$$

6. Similarly, the $\varphi^{m+1}(r)$ can be achieved by repetition of the above steps:

$$\varphi^{m+1}(r) = (N - m)^{-1} \sum_{i=1}^{N-m} \varphi_i^{m+1}(r). \tag{22}$$

7. Then the FuzzyEn of the time sequence is defined as:

$$FuzzyEn(m, r) = \lim_{N \to \infty} \big[\ln \varphi^m(r) - \ln \varphi^{m+1}(r)\big]. \tag{23}$$

8. Finally, for a finite N, calculate FuzzyEn by:

$$FuzzyEn(m, r, N) = \ln \varphi^m(r) - \ln \varphi^{m+1}(r). \tag{24}$$

The fuzzy function used in Eq. (7) was defined as:

$$\mu(d, r, n) = e^{-\left(\frac{d}{r}\right)^n}. \tag{25}$$

3.2. Global Fuzzy Entropy

The implementation of the subtraction of the average of the original signal segment in FuzzyEn leads to neglecting the signal's global fluctuation. Moreover, FuzzyEn is originally developed for the complexity assessment of the short-term physiological time series. On the other hand, the global characteristics of the bearing vibration signals may change with bearing conditions varying. Therefore, FuzzyEn might exhibit limitations when assessing the complexity of the bearing vibration signals. Based on the aforementioned consideration, the GFuzzyEn is employed to process the decomposition components after the raw bearing vibration signals are decomposed by the LMSST in this study. The main difference between GFuzzyEn and FuzzyEn is the construction of the m-dimensional vectors,[28] which is defined in GFuzzyEn as:

$$\mathbf{X}_i^m = \{u(i), u(i+1), \ldots, u(i+m-1)\} - \overline{u}_0(i),$$
$$1 \leq i \leq N - m + 1; \tag{26}$$

where $\overline{u}_0(i)$ is the mean of the whole time series:

$$\overline{u}_0(i) = N^{-1} \sum_{i=0}^{N-1} u(i). \tag{27}$$

3.3. Parameter Selection

Before computing GFuzzyEn, there are four parameters that need to be selected, i.e., m, r, N, and n. The embedding dimension m determines the detailed reconstruction of the dynamic process. Information loss will occur and a very large N ($10^m - 30^m$) is required if a large m is chosen. Generally, $m = 2$ is given. N is set to 4096 in this paper because the entropy values' calculation is influenced less by the data length. The parameters r and n determine the width and gradient of the fuzzy function boundary, respectively. According to the previous studies,[23,24,28] r is chosen on the basis of standard deviation (SD) and n should be given small integers. In this study, $r = 0.2SD$ is assigned and n is set to 2.

4. THE PROPOSED BEARING FAULT FEATURE EXTRACTION APPROACH

By combining the advantages of LMSST and GFuzzyEn, a new rolling bearing fault feature extraction method is put forward as follows.

1. Acquire the vibration data of a rolling bearing under different running states using an accelerometer.

2. The LMSST method is used to decompose the collected vibration signals of the rolling bearing and a number of modes are obtained. The first few modes containing abundant condition-related information are used for research.

3. The GFuzzyEn of the selected mode components is calculated, and the obtained entropy values are treated as bearing fault features of the reflecting various working conditions.

4. Finally, in order to further validate the performance of the proposed feature extraction method, the LMSST-GFuzzyEn features are employed to distinguish different bearing fault patterns and severities.

5. SIMULATION VALIDATION

In this section, the decomposition effectiveness of LMSST is validated by the simulated bearing fault signal under strong noise background. The simulated fault signal includes a natural frequency of 3000 Hz and the characteristic fault frequency is 100 Hz. A white Gaussian noise is added to the signal and the signal-to-noise ratio is 3, as shown in Fig. 1.

The bearing fault simulation signal is processed by the LMSST method. The first decomposition mode and the corresponding envelope spectrum are presented in Fig. 2, from which shows the decomposed component exhibit some obvious impacts and the envelope spectrum can clearly detect the characteristic fault frequency 100 Hz and its multiples of 2 and 3. The simulation analysis demonstrates that the LMSST method can extract the main fault information buried in the bearing vibration signal.
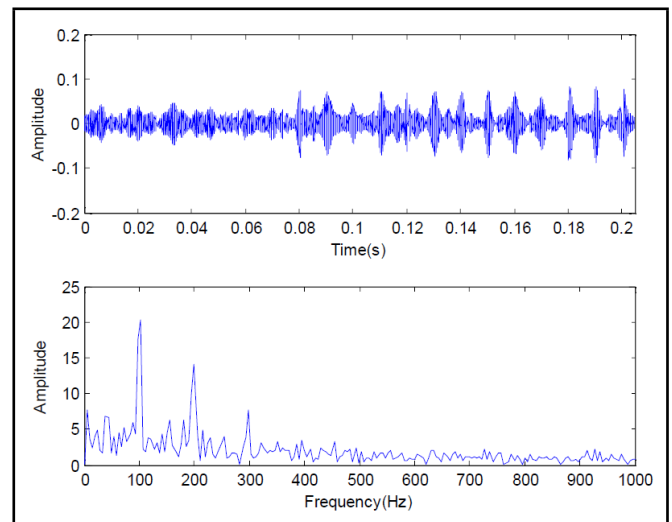
6. EXPERIMENTAL VALIDATION

6.1. Experimental Data

All the vibration data used for analysis in this study comes from the bearing data center of Case Western Reserve University.[32] The specific details about the experimental arrangement
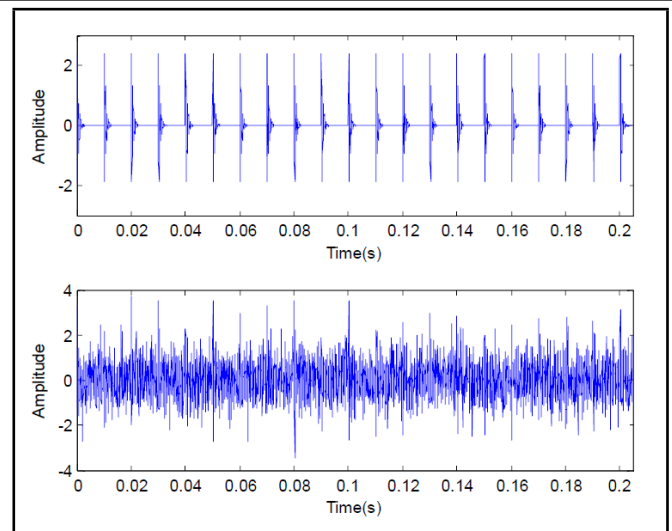
Figure 1. The bearing fault simulation signal (upper) and the signal with added noise (lower).

Figure 2. The decomposed component by LMSST (upper) and the envelope spectrum (lower).

can be found in the previous research.[18,20] The vibration signals under the speed of 1797 r/min with 0 horsepower load are analyzed for the experimental verification of the proposed approach. The description of the data in detail is illustrated in Table 1.

6.2. Results and Discussions

To verify the effectiveness of the proposed method, the fault feature extraction approach based on LMSST and GFuzzyEn is applied to the experimental bearing vibration data. For the seven bearing states, there are totally 203 data samples with 29 samples under each condition. Each data sample is obtained

Table 1. The detail of experimental data.

Bearing state	Fault size (mm)	Number of data samples	Label of classification
Normal	0	29	1
IRF1	0.1778	29	2
IRF2	0.5334	29	3
ORF1	0.1778	29	4
ORF2	0.5334	29	5
BF1	0.1778	29	6
BF2	0.7112	29	7

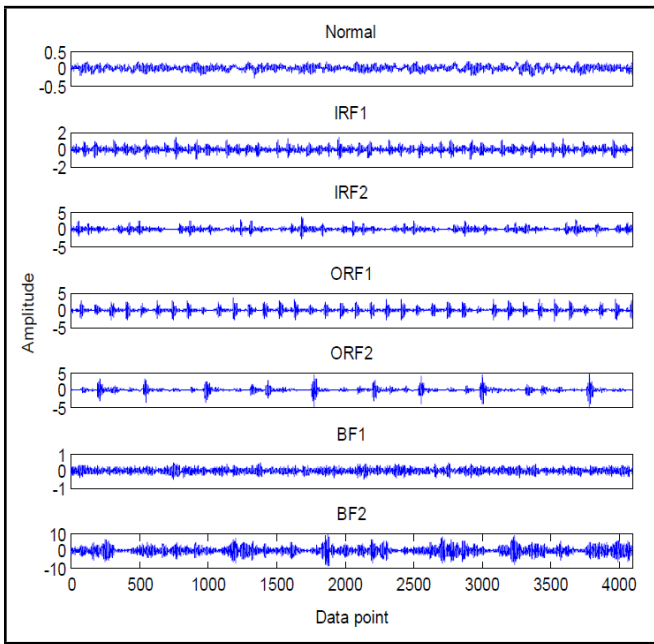**Figure 3.** Vibration signals of seven bearing conditions.
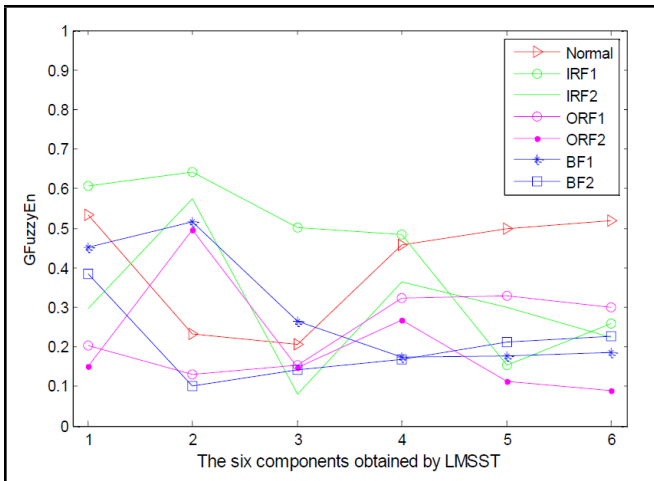
Figure 4. GFuzzyEn of the six components under seven bearing states.

Figure 5. The first two LMSST-GFuzzyEn features.
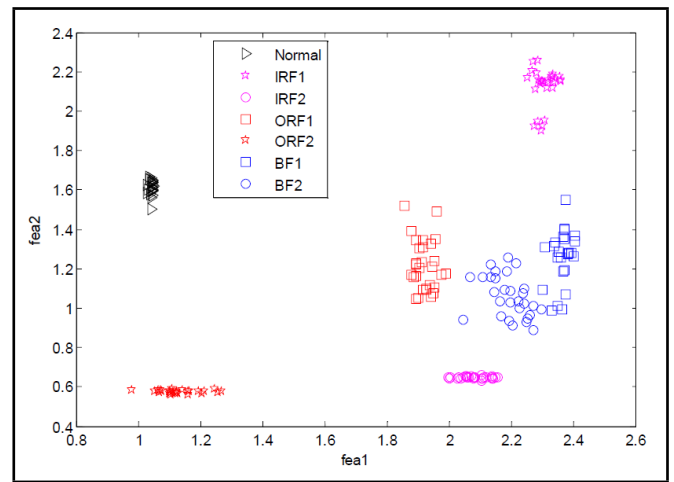
Figure 6. The first two LMSST-FuzzyEn features.

by truncation of a 4096-point segment with no overlapping between any two segments.

The typical bearing vibration signals' waveforms under seven different running states are plotted in Fig. 3, from which we can see that the vibration signals of different conditions present different traits. In order to extract the fault features from these vibration signals more effectively, further process is needed on the raw vibration data. Considering the time-varying characteristics of bearing vibration signals, in this study, LMSST and GFuzzyEn are combined to accomplish the bearing fault feature extraction from the vibration data due to their suitability of processing time-varying and nonlinear signals. The LMSST is first used to decompose the raw vibration signals into a group of modes. Then, the GFuzzyEn is applied to the obtained components. The six modes decomposed by LMSST are utilized for the calculation of GFuzzyEn.

Subsequently, the LMSST-GFuzzyEn features of the 203 data samples under seven bearing states can be obtained and a typical one is given in Fig. 4. From Fig. 4, it can be seen that the GFuzzyEn values of vibration signals of different condi-
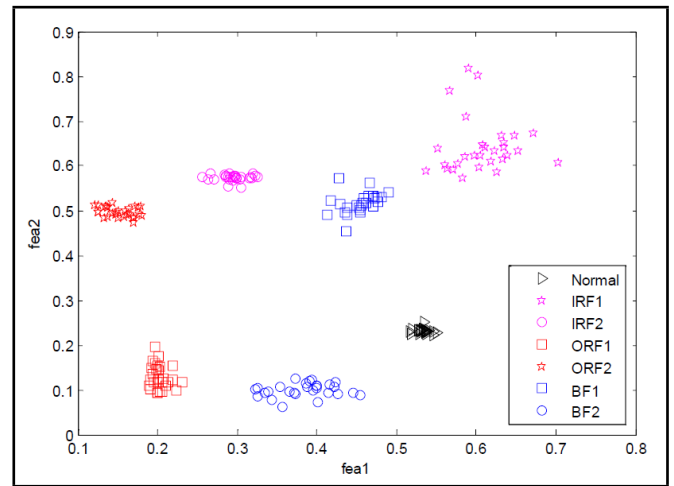
tions are different from each other over a variety of modes. Especially, the entropy values of the first two components exhibit apparent distinction. This is because the signals' complexity of different bearing states is different and thus the corresponding entropy value presents difference over various modes. To show the effectiveness of the LMSST-GFuzzyEn for bearing fault feature extraction, the visualizations of the first two features are illustrated in Fig. 5, from which we can see that the data samples of the same bearing condition show good clustering results and the samples of different categories separate from each other.

For comparison purpose, the EMD method and the empirical wavelet transform (EWT) method[33] are also utilized to decompose the bearing vibration signals. Correspondingly, the LMSST-FuzzyEn, EMD-GFuzzyEn and EWT-GFuzzyEn features are computed and the first two features of them are presented in Figs. 6–8, respectively. It can be seen from Fig. 6 that there is a slight overlapping between the data samples of BF1 and BF2 states. From Fig. 7, it can be observed that the overlapping phenomenon also exists and the data samples of IRF1 and BF1 demonstrate obvious overlapping. From Fig. 8, we can see that there is clear overlapping between the data samples of IFR1 and IRF2, and the data samples of ORF2 and BF1. This comparison shows that LMSST-GFuzzyEn can achieve the best clustering performance and implies that the LMSST-
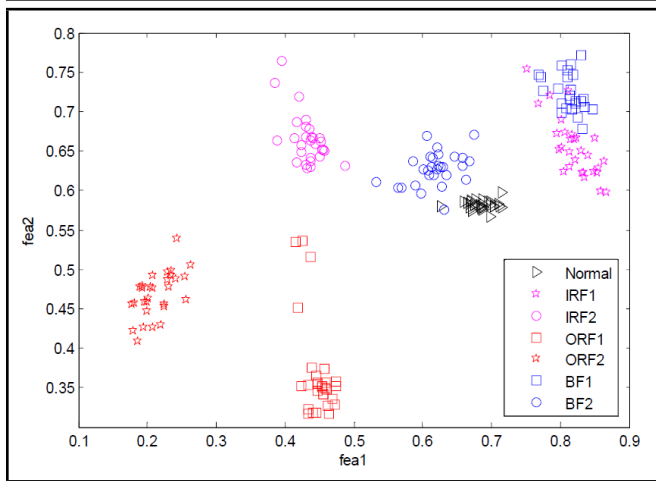
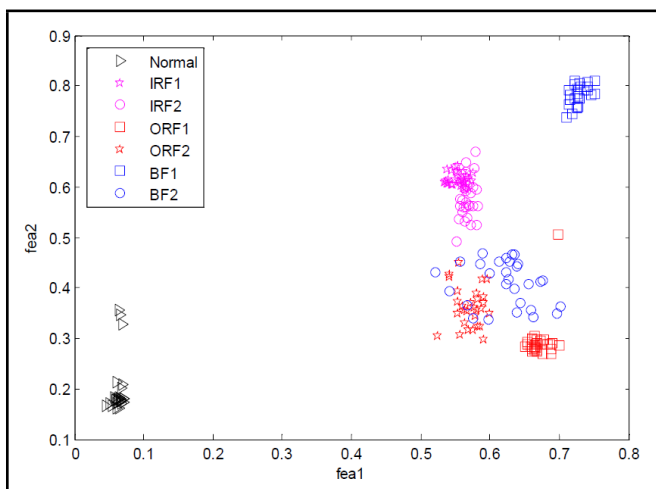**Figure 7.** The first two EMD-GFuzzyEn features.

Figure 8. The first two EWT-GFuzzyEn features.

GFuzzyEn features can extract more condition-reflecting information from the bearing vibration signals than those of LMSST-FuzzyEn, EMD-GFuzzyEn and EWT-GFuzzyEn.

To further verify the effectiveness of the proposed feature extraction approach, the multi-class SVM classifier is adopted for classification, which is implemented by LIBSVM[34] and radial basis function (RBF) kernel is selected owing to its merits.[35] The optimal selection of kernel parameter and penalty parameter in RBF-SVM is fulfilled using the five-fold cross-validation and grid search method. As previously mentioned, there are 203 data samples in total for seven bearing conditions. Among them, 14 samples of each class, a total of 98 samples are randomly chosen to train the SVM model and the remaining 105 samples are tested by the trained classifier. Similarly, to compare the classification performance of LMSST-GFuzzyEn with those of LMSST-FuzzyEn ,EMD-GFuzzyEn and EWT-GFuzzyEn, the latter three kinds of features are also used to train and test the SVM classifier. The classification results are shown in Table 2. As shown in Table 2, the LMSST-GFuzzyEn based method achieves the highest classification accuracy on both the training data set and the testing data set, which indicates that it has a better classification capability than the methods based on LMSST-FuzzyEn, EMD-GFuzzyEn and EWT-GFuzzyEn. This result is in accordance with the clustering performance of the three types of features analyzed above,

Table 2. Classification accuracy comparison based on different feature extraction methods.

| Method	Number of training samples	Number of testing samples	Number of misclassified training / testing samples	Training accuracies / testing accuracies (%)
LMSST + GFuzzyEn	98	105	0 / 0	100 / 100
LMSST + FuzzyEn	98	105	0 / 2	100 / 98.10
EMD + GFuzzyEn	98	105	6 / 4	93.88 / 96.19
EWT + GFuzzyEn	98	105	6 / 10	93.88 / 90.48

which further confirms the effectiveness and superiority of the LMSST-GFuzzyEn features in the rolling bearing fault diagnosis.

For the purpose of further comparison, the influence of the number of the features input into the SVM classifier on recognition results is investigated. The classification results are presented in Fig. 9 and Fig. 10. Figure 9 shows the identification rate of the training samples, from which it can be seen that the accuracy of the LMSST-GFuzzyEn method is not lower than those of the other three methods over all of the numbers of used features. The best training accuracy based on LMSST-GFuzzyEn can achieve 100% when the number of features is larger than 2. Figure 10 describes the recognition rate of the testing samples. From Fig. 10, it can be observed that over all of the feature numbers, the recognition accuracy based on the LMSST-GFuzzyEn method is higher than those based on the other three methods. The highest testing accuracy of the LMSST-GFuzzyEn method is 100% when the number of features used for classification is 2. This comparison further validates the effectiveness of the proposed LMSST-GFuzzyEn approach for the rolling bearing fault feature extraction.

From all the above analysis, it can be concluded that compared with LMSST-FuzzyEn, EMD-GFuzzyEn and EWT-GFuzzyEn, the proposed LMSST-GFuzzyEn exhibits the best fault feature extraction ability and can achieve the best classification performance for fault diagnosis of rolling bearings.

7. CONCLUSIONS

In this study, a rolling bearing fault feature extraction approach was put forward based on LMSST and GFuzzyEn. The LMSST algorithm was utilized to decompose the time-varying bearing vibration signals into a group of mode components. GFuzzyEn was employed to assess the complexity of the first several modes considering that the bearing vibration signals' global characteristics may change with working conditions of the rolling bearing varying. The experimental results show that the LMSST-GFuzzyEn features exhibit good clustering performance. Furthermore, in order to verify the effectiveness of the proposed LMSST-GFuzzyEn method for classification, the SVM multi-class classifier was adopted. As a contrast, the features of LMSST-FuzzyEn, EMD-GFuzzyEn and EWT-GFuzzyEn were also used to analyze the bearing vibration signals, respectively. The experimental analysis demonstrates that LMSST-GFuzzyEn showed a better bearing fault feature extraction capability than the other three kinds of features and obtained the best identification performance for a rolling bearing fault diagnosis. Compared with LMSST-FuzzyEn, the performance of LMSST-GFuzzyEn indicated that the GFuzzyEn could extract more fault information from the bearing vibration signals than FuzzyEn. The compari-
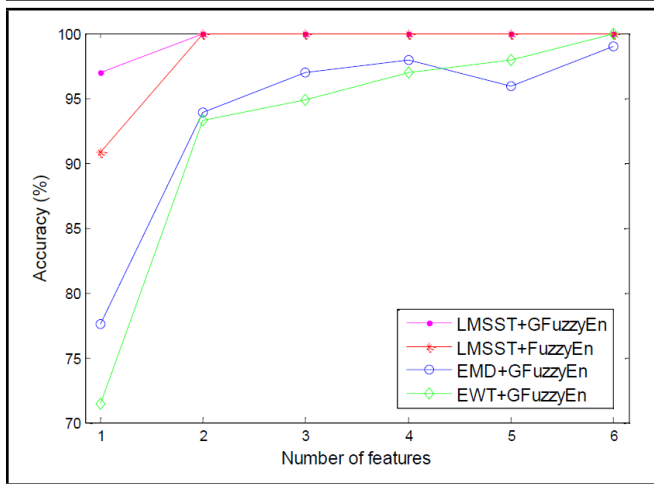
Figure 9. Recognition rate comparison of different feature extraction approaches with different number of features (training samples).
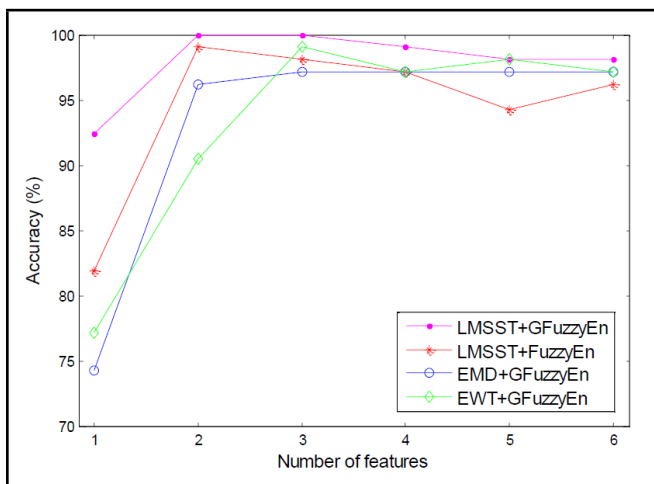
Figure 10. Recognition rate comparison of different feature extraction approaches with different number of features (testing samples).

son between LMSST-GFuzzyEn, EMD-GFuzzyEn and EWT-GFuzzyEn showed that LMSST may exhibit a better decomposition effect than EMD and EWT when dealing with the vibration signal of a rolling bearing. All the analyses manifest that LMSST-GFuzzyEn has its advantages and considerable potential in the rolling bearing fault diagnosis.

ACKNOWLEDGEMENTS

REFERENCES

1 Tiwari, R., Gupta, V. K., and Kankar, P. K. Bearing fault diagnosis based on multi-scale permutation entropy and adaptive neuro fuzzy classifier, *Journal of Vibration and Control*, **21**, 461–467, (2015). https://dx.doi.org/10.1177/1077546313490778

2 Kumar, A. and Kumar, R. Role of signal processing, modeling and decision making in the diagnosis of rolling element bearing defect: A review. *Journal of Nondestructive Evaluation*, **38**, 5, (2019). https://dx.doi.org/10.1007/s10921-018-0543-8

3 Li, Y. B., Wang, X. B., Si, S., and Huang, S. Entropy based fault classification using the Case Western Reserve University data: A benchmark study, *IEEE Transactions on Reliability*, **69**, 754–767, (2020). https://dx.doi.org/10.1109/TR.2019.2896240

4 Song, Y. and Wang, W. A fault feature extraction method for rolling bearings based on refined composite multi-scale amplitude-aware permutation entropy, *IEEE Access*, **9**, 71979–71993, (2021). https://dx.doi.org/10.1109/ACCESS.2021.3078823

5 Feng, Z. P., Ma, H., and Zuo, M. J. Vibration signal models for fault diagnosis of planet bearings, *Journal of Sound and Vibration*, **370**, 372–393, (2016). https://dx.doi.org/10.1016/j.jsv.2016.01.041

6 Zhang, X., Zhao, J., Li, H., Yang, R., and Teng, H. Rolling bearings fault diagnosis under variable conditions using RCMFE and improved support vector machine, *International Journal of Acoustics and Vibration*, **25** (3), (2020). https://dx.doi.org/10.20855/ijav.2020.25.31596

7 Dong, G. M., Chen, J., and Zhao, F. Incipient bearing fault feature extraction based on minimum entropy deconvolution and K-singular value decomposition, *Journal of Manufacturing Science and Engineering*, **139** (10), (2017). https://dx.doi.org/10.1115/1.4037419

8 Huang, N. E., Shen, Z., Long, S. R., Wu, M. C., Shih, H. H., Zheng, Q., Yen, N.-C., Tung, C. C., and Liu, H. H. The empirical mode decomposition and the Hilbert spectrum for nonlinear and non-stationary time series analysis, *Proceedings of the Royal Society A: Mathematical, Physical and Engineering Sciences*, **454**, 903–995, (1998). https://dx.doi.org/10.1098/rspa.1998.0193

9 Yang, Y., Yu, D. J., and Cheng, J. S. A roller bearing fault diagnosis method based on EMD energy entropy and ANN, *Journal of Sound and Vibration*, **294**, 269–277, (2006). https://dx.doi.org/10.1016/j.jsv.2005.11.002

10 Zair, M., Rahmoune, C., and Benazzouz, D. Multi-fault diagnosis of rolling bearing using fuzzy entropy of empirical mode decomposition, principal component analysis, and SOM neural network, *Proceedings of the Institution of Mechanical Engineers, Part C: Journal of Mechanical Engineering Science*, **233** (9), 3317–3328, (2019). https://dx.doi.org/10.1177/0954406218805510

11 Wang, J., Du, G., Zhu, Z., Shen, C., and He, Q. Fault diagnosis of rotating machines based on the EMD manifold, Mechanical Systems and Signal Processing, **135**, 106443, (2020). https://dx.doi.org/10.1016/j.ymssp.2019.106443

12 Feng, Z. P., Zhang, D., and Zuo, M. J. Adaptive mode decomposition methods and their applications in signal analysis for machinery fault diagnosis: A review with examples, *IEEE Access*, **5**, 24301–24331, (2017). https://dx.doi.org/10.1109/ACCESS.2017.2766232

13 Daubechies, I., Lu, J., and Wu, H. T. Synchrosqueezed wavelet transforms: An empirical mode decomposition-like tool, *Applied and Computational Harmonic Analysis*, **30**, 243–261, (2011). https://dx.doi.org/10.1016/j.acha.2010.08.002

14 Thakur, G. and Wu, H. T. Synchrosqueezing-based recovery of instantaneous frequency from nonuniform samples, *SIAM Journal on Mathematical Analysis*, **43**, 2078–2095, (2011). https://dx.doi.org/10.1137/100798818

15 Li, C., Sanchez, V., Zurita, G., Lozada, M. C., and Cabrera, D. Rolling element bearing defect detection using the generalized synchrosqueezing transform guided by time–frequency ridge enhancement, *ISA Transactions*, **60**, 274–284, (2016). https://dx.doi.org/10.1016/j.isatra.2015.10.014

16 Liu, W., Chen, W., and Zhang, Z. A novel fault diagnosis approach for rolling bearing based on high-order synchrosqueezing transform and detrended fluctuation analysis, *IEEE Access*, **8**, 12533–12541, (2020). https://dx.doi.org/10.1109/ACCESS.2020.2965744

17 Yu, G., Wang, Z. H., Zhao, P., and Li, Z. Local maximum synchrosqueezing transform: An energy-concentrated time-frequency analysis tool, *Mechanical Systems and Signal Processing*, **117**, 537–552, (2019). https://dx.doi.org/10.1016/j.ymssp.2018.08.006

18 Yan, R. and Gao, R. X. Approximate entropy as a diagnostic tool for machine health monitoring, *Mechanical Systems and Signal Processing*, **21**, 241–250, (2007). https://dx.doi.org/10.1016/j.ymssp.2006.02.009

19 Zhang, L., Xiong, G. L., and Liu, H. S. Bearing fault diagnosis using multi-scale entropy and adaptive neuro-fuzzy inference, *Expert Systems with Applications*, **37**, 6017–6085, (2010). https://dx.doi.org/10.1016/j.eswa.2010.02.118

20 Liu, H. H. and Han, M. H. A fault diagnosis method based on local mean decomposition and muti-scale entropy for roller bearings, *Mechanism and Machine Theory*, **75**, 67–78, (2014). https://dx.doi.org/10.1016/j.mechmachtheory.2014.01.011

21 Zhu, K. H. Performance degradation assessment of rolling element bearings based on hierarchical entropy and general distance, *Journal of Vibration and Control*, **24** (14), 3194–3205, (2018). https://dx.doi.org/10.1177/1077546317702030

22 Ge, J. H., Niu, T. Y., Xu, D., Yin, G., and Wang, Y. A rolling bearing fault diagnosis method based on EEMD-WSST signal reconstruction and multi-scale entropy, *Entropy*, **22**, 290, (2020). https://dx.doi.org/10.3390/e22030290

23 Li, Y. B., Xu, M. Q., Wang, R. X., and Huang, W. H. A fault diagnosis scheme for rolling bearing based on local mean decomposition and improved multiscale fuzzy entropy, *Journal of Sound and Vibration*, **360**, 277–299, (2016). https://dx.doi.org/10.1016/j.jsv.2015.09.016

24 Zheng, J. D., Cheng, J. S., Yang, Y., and Luo, S. R. A rolling bearing fault diagnosis method based on multi-scale fuzzy entropy and variable predictive model-based class discrimination, *Mechanism and Machine Theory*, **78**, 187–200, (2014). https://dx.doi.org/10.1016/j.mechmachtheory.2014.03.014

25 Bin, J., Zhang, H. J., Liu, Y. B., Liu, F., Lu, S., and Dai, Z. A feature extraction method using improved multi-scale entropy for rolling bearing fault diagnosis, *Entropy*, **20**, 212, (2018). https://dx.doi.org/10.3390/e20040212

26 Pincus, S. M. Approximate entropy as a measure of system complexity, *Proceedings of the National Academy of Sciences*, **88** (6), 2297–2301, (1991). https://dx.doi.org/10.1073/pnas.88.6.2297

27 Richman, J. S. and Moorman, J. R. Physiological time-series analysis using approximate entropy and sample entropy, *American Journal of Physiology—Heart and Circulatory Physiology*, **278**, H2039–H2049, (2000). https://dx.doi.org/10.1152/ajpheart.2000.278.6.H2039

28 Chen, W. T., Wang, Z. Z., Xie, H. B., and Yu, W. X. Characterization of surface EMG signal based on fuzzy entropy, *IEEE Transactions on Neural Systems and Rehabilitation Engineering*, **15** (2), 266–272, (2007). https://dx.doi.org/10.1109/TNSRE.2007.897025

29 Liu, C. Y., Li, K., Zhao, L. N., Liu, F., Zheng, D. C., Liu, C. C., and Liu, S. T. Analysis of heart variability using fuzzy measure entropy, *Computers in Biology and Medicine*, **43**, 100–108, (2013). https://dx.doi.org/10.1016/j.compbiomed.2012.11.005

30 Auger, F. and Flandrin, P. Improving the readability of time-frequency and time-scale representations by the reassignment method, *IEEE Transactions on Signal Processing*, **43**, 1068–1089, (1995). https://dx.doi.org/10.1109/78.382394

31 Ahrabian, A., Looney, D., Stanković, L., and Mandic, D. P. Synchrosqueezing-based time-frequency analysis of multivariate data, *Signal Processing*, **106**, 331–341, (2015). https://dx.doi.org/10.1016/j.sigpro.2014.08.010

32 The Case Western Reserve University bearing data center, https://engineering.case.edu/bearingdatacenter/download-data-file (Accessed 17.03.2022).

33 Deng, W., Zhang, S., Zhao, H., and Yang, X. A novel fault diagnosis method based on integrating empirical wavelet transform and fuzzy entropy for motor bearing, *IEEE Access*, **6**, 35042–35056, (2018). https://dx.doi.org/10.1109/ACCESS.2018.2834540

34 Chang, C. C. and Lin, C. F. LIBSVM: A library for support vector machines, *ACM Transactions on Intelligent Systems and Technology*, **2** (3), 1–27, (2011). https://dx.doi.org/10.1145/1961189.1961199

35 Widodo, A. and Yang, B. S. Support vector machine in machine condition monitoring and fault diagnosis, *Mechanical Systems and Signal Processing*, **21** (6), 2560–2574, (2007). https://dx.doi.org/10.1016/j.ymssp.2006.12.007